Solid State Communications 152 (2012) 1715–1718

Contents lists available at SciVerse ScienceDirect

Solid State Communications

journal homepage: www.elsevier.com/locate/ssc

Ultrasonic study on the Jahn–Teller effect near different phase transitions in $La_{1/3}Sr_{2/3}MO_3$ (M=Mn, Fe, Co)

Kong Hui [a,*], Zhu Changfei [b]

[a] School of Metallurgy and Resources, Anhui University of Technology, Maanshan, Anhui 243002, PR China
[b] Laboratory of Advanced Functional Materials and Devices, Department of Materials Science and Engineering, University of Science and Technology of China, Hefei, Anhui 230026, PR China

ARTICLE INFO

Article history:
Received 16 January 2012
Received in revised form
26 June 2012
Accepted 2 July 2012
by J. Fontcuberta
Available online 7 July 2012

Keywords:
A. Transition metal alloys and compounds
D. Electron–phonon interaction
D. Ultrasonic

ABSTRACT

The longitudinal ultrasonic velocity (V_l), magnetization and resistivity of polycrystalline $La_{1/3}Sr_{2/3}MO_3$ (M=Mn, Fe, Co) have been measured between 20 and 300 K. Dramatic anomalies in V_l were observed near the temperature of the charge-ordering transition (CO), charge disproportionation transition (CD), and ferromagnetic transition (FM), which are explained by the Jahn–Teller effect originating from the M ions (M=Mn, Fe, Co). However, the detailed form of these anomalies is different, which is strongly depended on the M ion's unique electronic structure. For $La_{1/3}Sr_{2/3}MO_3$ (M=Mn, Fe), the V_l exhibits a valley around the CO transition temperature because of the localization of the Jahn–Teller active ions (Mn^{3+}, Fe^{4+}). And due to the instability of Fe^{4+}, the CD transition occurs in $La_{1/3}Sr_{2/3}FeO_3$, which results in another softening in V_l, while only normal increase is observed in $La_{1/3}Sr_{2/3}MnO_3$. For $La_{1/3}Sr_{2/3}CoO_3$, the local lattice distortion via the Jahn–Teller effect of intermediate spin Co^{3+} leads to the velocity anomaly in the ferromagnetic metallic state.

1. Introduction

Since the discoveries of high-*Tc* cuprates [1] and colossal-magnetoresistive manganites [2], the Jahn–Teller effect has attracted much attention. This effect removes the orbital degeneracy and plays an important role in many interesting physical phenomena [3]. Thus, the understanding of Jahn–Teller effect is an important issue in the present studies and the systematic study of closely related Jahn–Teller systems is needed. The perovskite-type $La_{1/3}Sr_{2/3}MO_3$ (M=Mn, Fe, Co) are such specimens.

In $La_{1/3}Sr_{2/3}MO_3$ (M=Mn, Fe, Co), the transition-metal ions ($t_{2g}^3e_g^1$ configuration on high-spin Mn^{3+}, Fe^{4+} ions, and $t_{2g}^5e_g^1$ configuration on intermediate-spin Co^{3+}) all have one unpaired electron residing in the two-fold degenerate e_g level, and when the e_g electrons are localized, this degeneracy may be removed by a Jahn–Teller distortion. However, this Jahn–Teller effect was related to the different kinds of phase transitions though these compounds have the similar structure. For M=Mn, charge ordering (CO) accompanies antiferromagnetic (AFM) spin ordering [4]. And for M=Fe, CO accompanies both AFM ordering and charge disproportionation (CD) of $2Fe^{4+}\rightarrow Fe^{3+}+Fe^{5+}$ [5,6]. While in $La_{1/3}Sr_{2/3}CoO_3$, it shows metallic behavior in the whole temperature range [7]. Thus, a detailed comparison of the Jahn–Teller distortion in $La_{1/3}Sr_{2/3}MO_3$ (M=Mn, Fe, Co) may be helpful to elucidate the role of the Jahn–Teller effect.

As a sensitive tool, ultrasonic technique has been proven to be particularly successful in studying the Jahn–Teller effect in transition-metal oxides. Recently, the ultrasonic responses to the formation of the Jahn–Teller distortion in manganites and iron oxides have been theoretically and experimentally studied [8–13]. In this paper, we present a systematic study of longitudinal ultrasonic velocity (V_l) as a function of temperature in polycrystalline $La_{1/3}Sr_{2/3}MO_3$ (M=Mn, Fe, Co) in order to gain more insight into the relationship between the Jahn–Teller effect and different types of phase transitions.

2. Experimental procedure

To precisely measure the properties of $La_{1/3}Sr_{2/3}MO_3$ (M=Fe, Co), the single crystals are recommended. However, for perovskite-type transition-metal oxides, the single crystals are hard to get, especially the large bulk for ultrasonic measurement. Thus, in published papers [9–13], most samples are polycrystalline, which could qualitatively exhibit its ultrasonic property. For example, the first experimental evidence, which correlates the ultrasonic velocity anomaly with the Jahn–Teller effect in manganites, was published at PRL in 1996 [11]. Its experimental sample is polycrystalline, and the ultrasonic frequency is 10 M without using different waves polarizations. In 2012, the ultrasonic feature of

* Corresponding author. Tel.: +86 555 2315180.
E-mail address: konghui@ahut.edu.cn (K. Hui).

0038-1098/$ - see front matter © 2012 Elsevier Ltd. All rights reserved.
http://dx.doi.org/10.1016/j.ssc.2012.07.003

polycrystalline $(La_{0.6}Pr_{0.4})_{0.7}Ca_{0.3}MnO_3$ is published in PRB [13]. Moreover, based on the Hamiltonian of small polarons with strong electron–phonon coupling, Min et al. [8] also found that in manganites, the CO interaction induces the softening of the sound velocity above T_{CO} and the hardening below T_{CO}. Their calculation result is not based on the different waves polarizations. Thus, it is reasonable to use polycrystalline samples in our paper, and the analysis of ultrasonic feature is based on the solid foundation.

The polycrystalline samples of $La_{1/3}Sr_{2/3}MO_3$ (M=Fe, Co) were synthesized via a conventional solid-state reaction method. A stoichiometric mixture of high-purity La_2O_3, $SrCO_3$, Fe_2O_3 and Co_2O_3 powders were well mixed, ground and calcinated at 1000,1100,1200 °C in the air for 15 h, respectively. And the polycrystalline $La_{1/3}Sr_{2/3}MnO_3$ sample was synthesized by the chemical citrate-gel route. Stoichiometric amounts of aqueous metal nitrates were prepared by dissolving La_2O_3, $SrCO_3$ and $Mn(NO_3)_2$ in a minimum amount of concentrated nitric acid. After adding the citric acid, the pH value of solution is adjusted to 6–7. The solution was subsequently stirred and evaporated at 80 °C to form the polymeric precursor, which was ignited in air to remove the organic contents. The resulting ash was ground to fine powders and calcined at 800 °C in air for 10 h.

The final obtained powder was pressed into pellets at 300 MPa and then sintered at different temperature (1200 °C for Fe compound, 1250 °C for Co compound and 1500 °C for Mn compound) in air for 20 h, and cooled to room temperature at a rate of 1 °C min^{-1}.

The crystal structure was characterized using a Japan Rigaku MAX-RD powder X-ray diffractometer with Cu$K\alpha$ radiation (λ=1.5418 Å). The resistivity was measured by the standard four-probe technique. For $La_{1/3}Sr_{2/3}MO_3$ (M=Fe, Mn), the zero-field-cooled magnetization was measured in an external magnetic field of 100 Oe by a commercial quantum device (SQUID; Quantum Design MPMSXL). However, according to the previous studies, it's known that for $La_{1/3}Sr_{2/3}CoO_3$, the field cooled magnetization is more exact to demonstrate its ferromagnetic transition temperature (T_C) than the zero-field-cooled magnetization curve [7]. Thus, the sample of $La_{1/3}Sr_{2/3}CoO_3$ was initially cooled in 100 Oe to 5 K, and then the field cooled magnetization was measured under 100 Oe as the sample was heated up to 300 K by the SQUID.

The specimens for ultrasonic measurement were in the form of flat disk, 4.5–5.2 mm thick, and were hand-lapped to a parallelism of faces better than 2 parts in 10^4. The longitudinal ultrasonic velocity measurement was performed on the Matec-7700 oscillator/receiver series with a conventional pulsed echo technique. Longitudinal ultrasonic wave pulses are generated by an X cut quartz transducer at a frequency of 10 MHz. It was bonded to the sample surface with nonaqueous stopcock grease and converted the energy to ultrasound. All experiments were taken in a closed-cycle refrigerator during the warm-up from 20 to 300 K at the rate of about 0.25 K/min.

3. Experimental results and discussion

The X-ray diffraction patterns of the $La_{1/3}Sr_{2/3}MO_3$ (M=Mn, Fe, Co) are shown in Fig. 1. All samples are of single phase with no detectable secondary phases. The diffraction peaks are sharp and can be indexed in the pseudo-cubic structure.

The temperature dependences of resistivity and magnetization for $La_{1/3}Sr_{2/3}MO_3$ (M=Mn, Fe, Co) are shown in Fig. 2. For $La_{1/3}Sr_{2/3}MO_3$ (M=Mn, Fe), the resistivity shows semiconductive behavior over the entire temperature range. And a conspicuous increase in resistivity was observed near the charge ordering temperature T_{CO}, while the magnetization shows a cusp structure. This feature

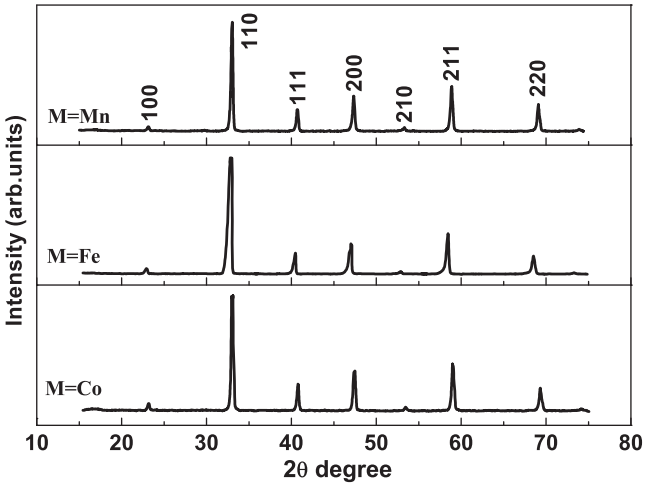

Fig. 1. XRD patterns of $La_{1/3}Sr_{2/3}MO_3$ (M=Mn, Fe, Co) at room temperature.

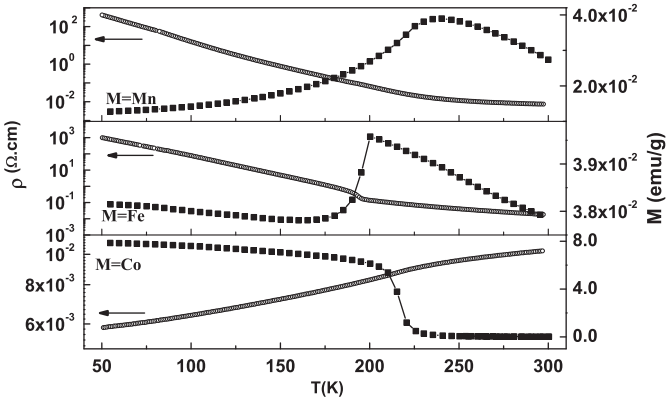

Fig. 2. Temperature dependences of resistivity and magnetization for $La_{1/3}Sr_{2/3}MO_3$ (M=Mn, Fe, Co).

implies the onset of the charge ordering state. For $La_{1/3}Sr_{2/3}MnO_3$, this ordering state is composed by the Mn^{3+} and Mn^{4+}. While for $La_{1/3}Sr_{2/3}FeO_3$, a sequence of …Fe^{3+} Fe^{3+} Fe^{5+} Fe^{3+} Fe^{3+} Fe^{5+}… exists along the [111] direction of the pseudocubic perovskite unit cell in this ordering state [14]. The difference between them is that the charge ordering transition in $La_{1/3}Sr_{2/3}FeO_3$ accompanies the CD transition of $2Fe^{4+} \rightarrow Fe^{3+} + Fe^{5+}$. However, this difference could not be distinguished through the resistivity and magnetization measurements.

The sample of $La_{1/3}Sr_{2/3}CoO_3$ shows metallic behavior in the whole temperature range and a kink around 230 K was observed, which coincides with the rapid increasing of the magnetization. Such a kink in resistivity is a common feature for $La_{1-x}Sr_xCoO_3$ because of the reduction of scattering from spin disorder in the FM state [15].

Fig. 3 exhibits the temperature dependence of ultrasonic velocity for $La_{1/3}Sr_{2/3}MO_3$ (M=Mn, Fe, Co). Different ultrasonic behaviors are observed near different kinds of transitions.

For Mn compound, the V_l softens smoothly as the temperature decreasing from 300 K and substantially increases below the T_{CO}, which exhibits a valley around T_{CO}. This feature is in good agreement with previous studies [8,9,11], and was attribute to the strong electron–phonon coupling via the Jahn–Teller effect of Mn^{3+}.

Compared with $La_{1/3}Sr_{2/3}MnO_3$, the ultrasonic feature in $La_{1/3}Sr_{2/3}FeO_3$ is rich. With decreasing temperature from 300 K, the V_l softens conspicuously, and there is a minimum around T_{CO}. It is well known that in the normal state, the ultrasonic velocity

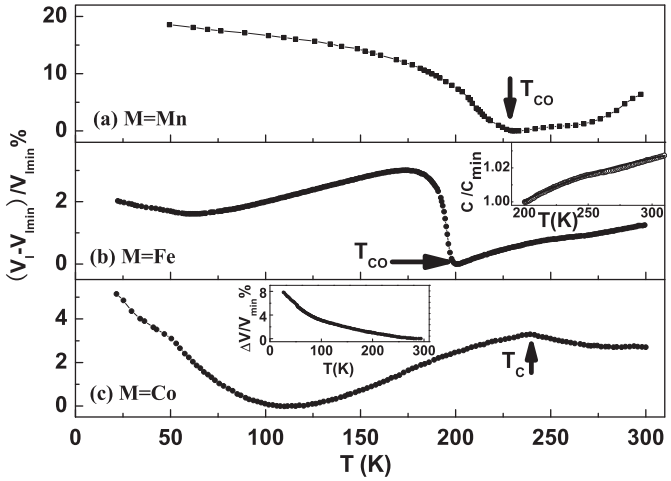

Fig. 3. The temperature dependence of the longitudinal ultrasonic velocity for $La_{1/3}Sr_{2/3}MO_3$ (M=Mn, Fe, Co) The inset of Fig. 3(b) is the temperature dependence of the C(T) for $La_{1/3}Sr_{2/3}FeO_3$ above T_{CO} (Open symbols are experimental data, solid line is the results calculated using Eq. (1)) The inset of Fig. 3(c) is the temperature dependence of the longitudinal ultrasonic velocity for $La_{0.8}Sr_{0.2}CoO_3$.

increases with the temperature decreasing. To investigate the origin of this ultrasonic anomaly, we have explored several possibilities.

The first consideration is the antiferromagnetic transition. According to the Landau–Khalatnilov theory, AFM ordering usually decreases the elastic stiffness due to the magnetostriction effect, and the relative softening in sound velocity is usually less than 0.1% [16]. While in $La_{1/3}Sr_{2/3}FeO_3$, the $\Delta V_l/V_{lmin}$ around T_{CO} is larger than 3%, which cannot be explained only based on spin-phonon coupling near a conventional AFM phase transition.

According to the acoustics theory, the softening in sound velocity is usually observed near the temperature of structural distortion or the formation of glassy state where, due to the weakening of certain force constants, a particular phonon mode softens [17]. Until now, no experimental evidence indicates that the spin-glass state exists in $La_{1/3}Sr_{2/3}FeO_3$. Thus, the similar ultrasonic feature between $La_{1/3}Sr_{2/3}MnO_3$ and $La_{1/3}Sr_{2/3}FeO_3$ around T_{CO} implies that the lattice distortion originated from the electron–phonon coupling may also play an important role for the CO transition in $La_{1/3}Sr_{2/3}FeO_3$. Moreover, based on the Hamiltonian of small JT polarons with strong electron–phonon coupling, Min et al. found that in manganites, the CO interaction induces the softening of V above T_{CO} and the hardening below T_{CO} [8]. This result is qualitatively similar to our observation.

According to the Jahn–Teller theory, the relationship between the longitudinal modulus C(T) and temperature T ($T > T_{CO}$) can be written as [18]:

$$C(T) = C_0(T-T_C^0)/(T-\Theta) \quad (1)$$

where $C(T)=\rho V_l^2$ [19], ρ is the mass density, C_0 is the elastic modulus in the absence of Jahn–Teller coupling of the lattice with the electronics state of the ions, and the characteristic temperature of T_C^0 and Θ can be determined by the ultrasonic measurements of the elastic modulus softening.

Eq. (1) can be used to fit the experimental data in the temperature range above T_{CO}. In the inset of Fig. 3(b), the open symbols are the experimental data and the solid line is the theoretical result (the values of the T_C^0, Θ, C_0/C_{min} are 49.55 K, 39.69 K, 1.066). The good agreement between experiment and theory indicates that the electron–phonon coupling via the Jahn–Teller effect indeed exists in $La_{1/3}Sr_{2/3}FeO_3$.

However, it is noticeable that the relative velocity change of $La_{1/3}Sr_{2/3}MnO_3$ is more than 10%, while that of $La_{1/3}Sr_{2/3}FeO_3$ is only about 3%. In manganites, the relative stiffening of the ultrasonic velocity ($\Delta V/V$) can be viewed as a scale of the development of the Jahn–Teller effect [20]. Thus, the small velocity change in $La_{1/3}Sr_{2/3}FeO_3$ implies that its Jahn–Teller effect is very weak. This result may explain the fact that the structural changes in $La_{1/3}Sr_{2/3}FeO_3$ cannot be observed through the neutron powder diffraction [14], while they can be observed through the powder x-ray diffraction measurement in charge ordered manganites [9]. This behavior is due to the instability of Fe^{4+}.

For Fe^{4+}, its electronic structure is a mixture of $3d^4$ and $3d^5\underline{L}$ ($\underline{L}$ denotes a hole in the O 2p band), and dominated by the $3d^5\underline{L}$ configuration [21]. This structure decreases the content of high-spin Fe^{4+} ($3d^4$). Thus the Jahn–Teller effect weakens and the resulting relative stiffening of ultrasonic velocity is small. In fact, the instability of Fe^{4+} also leads to the charge disproportionation transition. In $La_{1/3}Sr_{2/3}FeO_3$, the concentration of Fe^{4+} is larger than that of Fe^{3+}, thus two Fe^{4+} ions would neighbor when they localize. This would weaken the hybridization of the middle O 2p bands and make the charge ordering state unstable. To avoid this situation, the charge disproportionation of $2Fe^{4+} \rightarrow Fe^{3+}+Fe^{5+}$ occurs and a charge ordered sequence of $\ldots Fe^{3+}Fe^{5+}Fe^{3+}\ldots$ was found [3]. It is worth noting that that this CD transition lasts a temperature range [6]. Since Fe^{5+} cations occupy smaller octahedral sites than Fe^{3+} cations, it will result in the breathing-type distortion of Fe–O octahedron, which was confirmed by the measurements of transmission electron microscopy [5] and optical spectroscopy [22]. According to the ultrasonic theory, the lattice distortion can lead to the softening in sound velocity [14]. For example, the ultrasonic velocity softening was observed in Terbium, which originates from the rhombic distortion of the crystal lattice [23]. So below T_{CO}, another softening in ultrasonic velocity of $La_{1/3}Sr_{2/3}FeO_3$ was observed in Fig. 3, which is attributed to the breathing-type distortion.

It should be mentioned that due to the speciality of Fe^{4+}, the lattice distortion around CO–CD transitions in $La_{1/3}Sr_{2/3}FeO_3$ is still under discussion, and different conclusions have been drawn through different experimental and theoretical tools. First, no structural changes accompany the CO–CD transition [14,24]. Second, only breathing-type distortion of Fe–O octahedron exists below T_{CO} [5,22]. Third, the lattice distortions are present only above T_{CO} [25]. While from our analysis of ultrasonic feature, two kinds of lattice distortion are confirmed. The former is due to the dynamic Jahn–Teller effect and leads to the ultrasonic anomaly around T_{CO}. The latter is attributed to the breathing-type distortion and results in another softening in ultrasonic velocity below T_{CO}.

For $La_{1/3}Sr_{2/3}CoO_3$, it undergoes the FM transition at 230 K and shows the metallic behavior in the whole temperature range. This feature has been observed in previous works and is typically interpreted in terms of the ferromagnetic cluster model [26]. And the ferromagnetic clusters are dominated by the ferromagnetic double exchange interaction between Co^{3+} and Co^{4+}. Based on the Hamiltonian of small polarons with strong electron–phonon coupling, Min et al. [8] found that in manganites, the double exchange interaction induces the hardening of V_l below T_C. This conclusion was proven by the observation of Ramirez et al. for $La_{0.67}Ca_{0.33}MnO_3$ [11]. However for $La_{1/3}Sr_{2/3}CoO_3$, upon cooling down from T_C, the velocity softens conspicuously and stiffens dramatically below 120 K. Thus it seems impossible to correlate these ultrasonic anomalies with the magnetic transition.

According to the ultrasonic theory, structural distortion or the formation of glassy state may lead to the softening of sound velocity [17]. Thus, to compare the ultrasonic anomalies in $La_{1/3}Sr_{2/3}CoO_3$ with that caused by a typical glassy state in similar cobalt perovskite, we performed the temperature dependence of

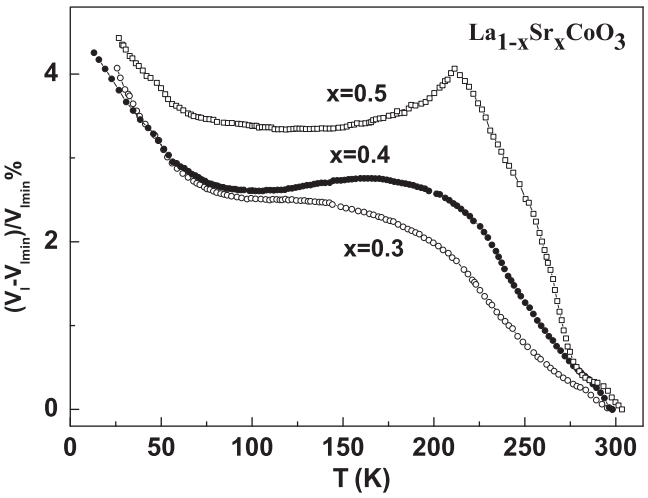

Fig. 4. The temperature dependence of the longitudinal ultrasonic velocity for $La_{1-x}Sr_xCoO_3$ ($x=0.3$, 0.4, 0.5).

the ultrasonic velocity for $La_{0.8}Sr_{0.2}CoO_3$ whose ground state is a cluster glassy state [27] (Inset of Fig. 3(c)). It can be seen that the sound velocity increases steadily with the temperature decreasing, and no softening is observed in the whole temperature range. This ultrasonic property is totally different from that of $La_{1/3}Sr_{2/3}CoO_3$. So the glassy state is not the origin of this ultrasonic anomaly and the local lattice distortion may be an alternative mechanism.

In $La_{1/3}Sr_{2/3}CoO_3$, the intermediate spin state ($t_{2g}^5e_g^1$, IS) of Co^{3+} is stabilized by the neighboring Co^{4+} through the size effects and covalency, thus it is Jahn–Teller active due to the double degeneracy of the e_g orbitals and may be respond to the ultrasonic anomalies in $La_{1/3}Sr_{2/3}CoO_3$ at low temperature. In fact, this local static lattice distortions have been observed in $La_{1-x}Sr_xCoO_3$ ($x>0.3$) by Louca et al. [28] from the pair density function analysis of neutron diffraction data.

It is worth noting that this Jahn–Teller effect occurs in the ferromagnetic metal state. This is strange since the itinerant electrons would make the localized lattice distortion unstable. According to the Louca's analysis [28], this is due to the fact that in $La_{1/3}Sr_{2/3}CoO_3$, the concentration of charges is so high that propagation occurs through well connected Co^{4+} without destroying the Jahn–Teller effect at some IS Co^{3+} sites. For a cubic lattice, the site percolation limit is 0.31 [29]. So in $La_{1-x}Sr_xCoO_3$, the static Jahn–Teller distortions only appear for $x>0.3$, which beyond the site percolation limit. This fact was confirmed by the pair density function analysis by Louca et al. [28].

To verify Louca's conclusion, we measured the V_l of $La_{1-x}Sr_xCoO_3$ ($x=0.3$, 0.4, 0.5) (shown in the Fig. 4). With increasing the Sr concentration, more Co^{4+} ions are induced and more intermediate spin state Co^{3+} ions will be localized without participating the double exchange. Thus the lattice distortions originating from the Jahn–Teller effect of Co^{3+} would be larger, which can be seen from the ultrasonic feature at low temperature. From the Fig. 4, it can be seen that the ultrasonic velocity softening becomes more obvious with increasing the Sr concentration. This fact is consistent with our above analysis and indicates that Jahn–Teller effect indeed exists in the high Sr-doping $La_{1-x}Sr_xCoO_3$.

4. Conclusion

In summary, we have systemically studied the ultrasonic properties of polycrystalline $La_{1/3}Sr_{2/3}MO_3$ (M=Mn, Fe, Co). Different ultrasonic anomalies are observed near different kinds of phase transitions in these samples, which can be explained by the Jahn–Teller effect originating from the transition-metal ions (M=Mn, Fe, Co). For $La_{1/3}Sr_{2/3}MO_3$ (M=Mn, Fe), the charge ordering transition leads to the localization of the Jahn–Teller active transition-metal ions ($t_{2g}^3e_g^1$ configuration on high-spin Mn^{3+}, Fe^{4+} ions), which makes the ultrasonic velocity exhibit a valley around T_{CO}. And due to the instability of Fe^{4+}, the CD transition occurs in $La_{1/3}Sr_{2/3}FeO_3$. Thus, the V_l of $La_{1/3}Sr_{2/3}FeO_3$ undergoes another softening transition, while normal increase is observed in $La_{1/3}Sr_{2/3}MnO_3$. For $La_{1/3}Sr_{2/3}CoO_3$, though the double exchange mechanism occurs in the ferromagnetic metallic state, the Jahn–Teller effect at the intermediate spin state Co^{3+} sites still exist, which results in the velocity anomaly below T_C. It can be seen that the detailed form of the ultrasonic anomalies is strongly depended on the transition-metal ion's electronic structure. These results may be helpful in understanding their unique electronic and magnetic properties.

Acknowledgment

This work was supported by the National Natural Science Foundation of China (no. 11004002).

References

[1] J.G. Bednorz, K.A. Műller, Z. Phys. B 64 (1986) 189–193.
[2] C.N.R. Rao, B. Raveau, Colossal Magnetoresistance, Charge Ordering and Related Properties of Manganese Oxides, World Scientific, Singapore, 1998.
[3] J.B. Goodenough, Mater. Res. Bull. 6 (1971) 967–976.
[4] Tetsuo Hiroyuki Fujishiro, Manabu Ikebe Fukase, J. Phys. Soc. Jpn. 67 (1998) 2582–2585.
[5] J.Q. Li, Y. Matsui, S.K. Park, Y. Tokura, Phys. Rev. Lett. 79 (1997) 297–300.
[6] J.B. Yang, X.D. Zhou, Z. Chu, W.M. Hikal, Q. Cai, J.C. Ho, D.C. Kundaliya, W.B. Yelon, W.J. James, H.U. Anderson, H.H. Hamdeh, S.K. Malik, J. Phys.: Condens. Matter 15 (2003) 5093–5102.
[7] J. Wu, C. Leighton, Phys. Rev. B. 67 (2003) 174408–174423.
[8] B.I. Min, J.D. Lee, S.J. Youn, J. Magn. Magn. Mater. 171 (1998) 881–883.
[9] X.-G. Li, H. Chen, C.F. Zhu, H.D. Zhou, R.K. Zheng, J.H. Zhang, L. Chen, Appl. Phys. Lett. 76 (2000) 1173–1175.
[10] H. Kong, C.F. Zhu, Europhys. Lett. 86 (2009) 54001–54005.
[11] A.P. Ramirez, P. Schiffer, S.-W. Cheong, C.H. Chen, W. Bao, T.T.M. Palstra, P.L. Gammel, D.J. Bishop, B. Zegarski, Phys. Rev. Lett. 76 (1996) 3188–3191.
[12] L. Jiang, J.R. Su, H. Kong, Y. Liu, S.-Y. Zheng, C.F. Zhu, J. Phys.: Condens. Matter 18 (2006) 8563–8571.
[13] M. Michelmann, V. Moshnyaga, K. Samwer, Phys. Rev. B. 85 (2012) 014424–014428.
[14] P.D. Battle, T.C. Gibb, P. Lightfoot, J. Solid State Chem. 84 (1990) 271–279.
[15] M.A. Seňarís-Rodríguez, J.B. Goodenough, J. Solid State Chem. 118 (1995) 323–336.
[16] D. Berlincourt, H. Jaffe, Phys. Rev. 111 (1958) 143–148.
[17] C.W. Garland, in: W.P. Maston, R.N. Thurston (Eds.), Physical Acoustics, vol. 7, Academic, New York, 1970, p. 52.
[18] R.L. Melcher, in: W.P. Maston, R.N. Thurston (Eds.), Physical Acoustics, vol. 12, Academic, New York, 1970, pp. 1–21.
[19] M. Cankurtaran, G.A. Saunders, K.C. Goretta, R.B. Poeppel, Phys. Rev. B 46 (1992) 1157–1165.
[20] R.K. Zheng, G. Li, Y. Yang, A.N. Tang, W. Wang, T. Qian, X.G. Li, Phys. Rev. B 70 (2004) 014408–014414.
[21] M. Abbate, F.M.F. de Groot, J.C. Fuggle, A. Fujimori, O. Strebel, F. Lopez, M. Domke, G. Kaindl, G.A. Sawatzky, M. Takano, Y. Takeda, H. Eisaki, S. Uchida, Phys. Rev. B 46 (1992) 4511–4519.
[22] S.K. Park, T. Ishikawa, Y. Tokura, J.Q. Li, Y. Matsui, Phys. Rev. B 60 (1999) 10788–10795.
[23] M. Rosen, Phys. Rev. 174 (1968) 504–514.
[24] J. Matsuno, T. Mizokawa, A. Fujimori, K. Mamiya, Y. Takeda, S. Kawasaki, M. Takano, Phys. Rev. B 60 (1999) 4605–4608.
[25] S. Ghosh, N. Kamaraju, M. Seto, A. Fujimori, Y. Takeda, S. Ishiwata, S. Kawasaki, M. Azuma, M. Takano, A.K. Sood, Phys. Rev. B 71 (2005) 245110–245116.
[26] S. Mukherjee, R. Ranganathan, P.S. Anilkumar, P.A. Joy, Phys. Rev. B 54 (1996) 9267–9274.
[27] M. Itoh, I. Natori, S. Kubota, K. Motoya, J. Phys. Soc. Jpn. 67 (1998) 1486–1493 1486 (1994).
[28] D. Louca, J.L. Sarrao, Phys. Rev. Lett. 91 (2003) 155501–155504.
[29] R. Zallen, The Physics of Amorphous Solids, Wiley, NewYork, 1983, pp.170.